Shape transitions and shape stability of giant phospholipid vesicles in pure water induced by area-to-volume changes

J. Käs and E. Sackmann
Physik Department (Biophysik E22), Technische Universität München, James-Franck-Straße, D-8046 Garching, Germany

ABSTRACT Shape transformations of vesicles of dimyristoylphosphatidylcholine (=DMPC) and palmitoyloleylphosphatidylcholine (=POPC) in ion-free water were induced by changing the area-to-volume ratio via temperature variations. Depending on the pretreatment we find several types of shape changes for DMPC (in pure water) at increasing area-to-volume ratio: (*a*) budding transitions leading to the formation of a chain of vesicles at further increase of the area-to-volume ratio, (*b*) discocyte-stomatocyte transitions, (*c*) reentrant dumbbell-pear-dumbbell transitions, and (*d*) spontaneous blebbing and/or tether formation of spherical vesicles. Beside these transitions a more exotic dumbbell-discocyte transition (*e*) was found which proceeded via local instabilities. Pears, discocytes, and stomatocytes are stable with respect to small temperature variations unless the excess area is close to values corresponding to limiting shapes of budded vesicles where temperature variations of ≤ 0.1°C lead to spontaneous budding to the inside or the outside. For POPC we observed only budding transitions to the inside leading either to chains of vesicles or to distributions of equally sized daughter vesicles protruding to the inside of the vesicle. Preliminary experiments concerning the effect of solutes are also reported. The first three types of shape transitions can be explained in terms of the bilayer coupling model assuming small differences in thermal expansivities of the two monolayers. This does not hold for the observed instabilities close to the limiting shapes.

INTRODUCTION

Fluctuations and shape transitions of fluid bilayer vesicles are studied for two reasons: firstly they provide insight into the physical basis of changes of cellular topology during many cellular processes such as the budding-fission-fusion sequence effecting the transport of vesicles from the endoplasmatic reticulum of a cell to the plasma membrane or the uptake of macromolecular aggregates via coated pits or phagocytosis (1). Secondly they provide insight into the properties of hyperelastic shells.

Interest in shape transformation has been greatly stimulated by the recent progress in theoretical models of fluid bilayers (2–5) which are essentially based on the Helfrich curvature elasticity model of fluid membranes.

In the original approach of Deuling and Helfrich (6) the shape changes were described in terms of the spontaneous curvature concept. A modified approach was adopted by Svetina and Zeks (2) which is based on the assumption that the shape of a vesicle is determined by the area-to-volume ratio (this is also an assumption in the Deuling and Helfrich model) and the area difference between the opposing monolayers. Although this so-called bilayer coupling model is related to the Helfrich model by a Legendre transformation it leads to different results concerning the order of the shape transitions and the routes of transition induced by variation of the area-to-volume ratio or by osmotic pressure differences. The original phase diagram proposed by Svetina and Zeks has been recently expanded by Seifert et al. (4). It represents the shapes of minimum bending energy as a function of the area-to-volume ratio and the area difference between the two monolayers.

The present experiments were first motivated by these new theoretical developments and secondly by conflicting experimental results. Some years ago it was shown in this laboratory that vesicles containing a charged lipid can undergo continuous transitions from a biconcave to an inside-budded shape via the stomatocyte shape or to an outside budded shape via the pear shape. More recently it was reported for the case of SOPC that small increases of the excess area already result in a discontinuous blebbing transition (7). Because the question arises whether these conflicting results are due to the use of charged lipids or to the use of additional solutes in the inner and outer aqueous phases, we reinvestigated the shape transitions of simple systems such as dimyristolphosphatidylcholine (DMPC) and palmitoyloleylphosphatidylcholine (POPC) in deionized (Millipore) water. The shape transitions were induced by variations of the excess area via temperature changes, making use of the high thermal expansivity of the bilayer in the fluid L_α-phase. Some preliminary studies concerning the influence of the solute ionic strength and the chemical asymmetry of the aqueous phases (at equal osmolarities) are also presented. We show that these simple systems can exhibit slow shape transitions (type

0006-3495/91/10/825/20 $2.00

1, 2, 3) or spontaneous transitions such as the sudden formation of tethers and blebs (type 4). In addition, we provide evidence that for a given change in temperature the type of transition may depend on the pretreatment of the vesicles. Moreover we found that the stomatocyte-shaped and pear-shaped vesicles become unstable very close to the limiting shapes (that is the inside- and outside-budded vesicles, respectively).

The shape transitions of type 1, 2, and 3 are quantitatively explained in terms of the bilayer coupling model by assuming a small difference in thermal expansivities of the two opposing monolayers. It should be pointed out, however, that the instability of the stomatocyte and pear-shaped vesicles cannot be explained in terms of the bilayer coupling model. A preliminary report of the present experiments was already given (8).

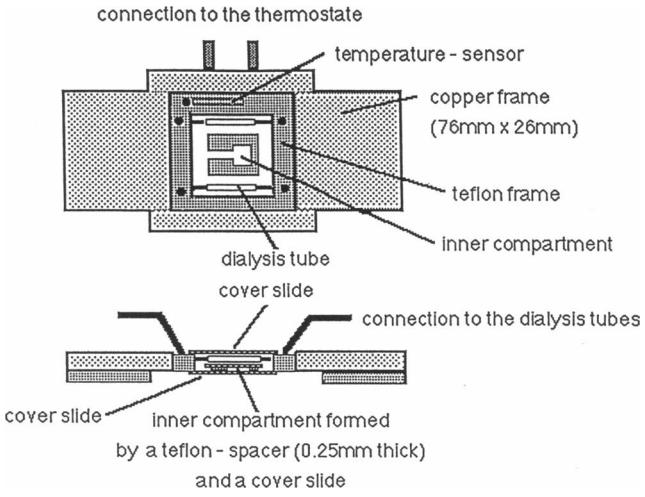

FIGURE 1 Measuring chamber with inner (deadwater) confinement to prevent swimming away of freely suspended vesicles by thermal convection. The chamber consists of a teflon frame ($3 \times 3 \times 0.4$ cm^3) tightly covered by cover glasses. It is filled into a copper block $0.76 \times 2.6 \times 0.5$ cm which is perforated by water for temperature variation. Temperature measurement occurs within the teflon frame by a Pt100 sensor. Two dialysis tubes (diameter $d = 0.9$ mm) are inserted into the chamber as indicated to change the osmolarity of the outer medium. The inner confinement consists of a rectangular teflon spacer of height 0.25 mm which is open on one side and is covered by a cover glass (1.4×1.2 cm^2) or a dialyze membrane of the same size. The copper-block was situated onto a teflon frame.

MATERIALS AND METHODS

Materials

L-α-dimyristoylphosphatidylcholine (DMPC) of purity better than 99% was purchased from Sigma Chemical Co. (St. Louis, MO). In vesicles, it exhibits a transition temperature of 23.8°C. *L*-α-Palmitoyl-oleoylphosphatidylcholine (POPC) of purity > 99% was obtained from Avanti Polar Lipids Inc. (Birmingham, AL). The transition temperature is ~5°C.

Vesicle preparation

For the preparation of giant vesicles the swelling procedure of Evans and Kwok was applied (9). The lipid was dissolved in chloroform methanol 2:1 (at a concentration of 10^{-3} M). 40 μl of the solution (containing $4 \cdot 10^{-8}$ mol of lipid) were deposited as a thin layer onto a roughened teflon disc which was placed onto the bottom of a glass beaker. Before use the beaker was carefully cleaned with Hellmanex (Hellma GmbH & Co., Müllheim Baden, Germany) and rinsed with high purity (Millipore) water. If used for the first time the beaker was filled with Millipore water for some days to remove ions. After solvent evaporation for 24 h, the beaker was filled with 4 ml Millipore water (or an aqueous solution) tightly covered by parafilm to avoid water evaporation and kept at 42°C for a minimum of 6 h. The formation of good vesicles is indicated by the appearance of schlieren. Small aliquots of the vesicle suspension were pipetted into the inner compartment of the measuring chamber (cf. Fig. 1). Then also the outer compartment was filled with the vesicle suspension.

Measuring chamber, microscope, and imaging

Our main concern was long time observation of vesicles swimming in the measuring chamber. For that purpose a temperature-controlled measuring chamber (shown in Fig. 1) was constructed where the vesicles could be kept in a confinement free of thermal convection. In the inner compartment, convection was sufficiently suppressed to keep the vesicle chosen within focus for several hours. The very slow lateral and vertical drift of the vesicle could easily be compensated manually. Heating and cooling was performed very slowly at rates of ≈ 0.2 K/min to always be close to thermal equilibrium. For a closer examination of the stability of vesicle shapes the temperature was changed in steps of 0.1 K and the vesicles were visualized for ~15 min after each step. The vesicles were observed by phase contrast microscopy using a Zeiss Axiovert 10 inverted microscope, equipped with a phase contrast air objective of magnification ×40 (Zeiss 40 × Ph2 nA = 0.75) with a large working distance of 400 μm and a numerical aperture of 0.75. For documentation the microscope was equiped with a CCD-camera (HR 480 Aqua TV, Kempten, Germany) with 604 × 588 pixels and a video recorder (Sony U-Matic, V05800 PS).

Two important questions are whether the vesicles are unilamellar and whether the vesicles are free from contact with the glass surface (e.g., via tethers). The latter problem was solved by transferring the giant vesicles to the inner confinement of the measuring chamber and by analyzing only freely swimming vesicles. In our knowledge, there is no way of absolute measurement of shell thicknesses. But high precision measurements of the bending stiffness, K_c, of vesicles by Fourier analysis of contour fluctuations showed that it is well possible to distinguish between vesicles of different lamellarity and that the majority of vesicles (typically ~75%) belongs to the group with the lowest value of K_c which is most likely unilamellar. Moreover because we observe one vesicle at a time over a time period of several hours, individual thick-walled vesicles would be sorted out by density sedimentation. If a vesicle is, for example, double walled its bending modulus is only twice as large as for a single walled vesicle. This should not effect the shape with the minimum bending energy.

Measurement of area and volume of vesicles

Area A and volume V of the vesicles (exhibiting rotational symmetry) were determined during the temperature scan as follows: for spherical

shapes, the values were obtained simply by measurement of the vesicle radius, and for ellipsoidal shapes from measurements of the dimensions of the principal axes. For other shapes the following approach was adopted. The orientation of the rotational symmetry axis was determined by changing the focus in the vertical direction. As shown in the example of Fig. 2, the overall shape and symmetry of the vesicles could be reliably determined in this way. Since the vesicles exhibited slow rotational diffusion, one situation with a horizontal orientation of the rotational axis was always encountered (within ≤ 5 min). For these situations, the coordinates of the contour of the vesicles were determined by the image processing system described earlier (10). From these data, A and V were calculated by numerical integration. Then mean values of A and V were obtained by averaging a sequence of four images. The accuracy of this method was 1.5% for measurements of the area and 2% for those of the volume. This error was much smaller than the changes in area within the temperature range studied. It was just about sufficient to detect volume changes such as caused by local instabilities (c.f. example of Fig. 9 *b*).

EXPERIMENTAL RESULTS

Most of the experiments were performed with DMPC vesicles in pure water. The excess area, A_{excess}, of the shell (A_{excess} is the difference between the actual area and that which would be required to form a sphere of the same volume) was varied by changing the temperature. If not explicitly noted the changes in volume were negligible. In the following the major types of shape changes observed are summarized.

Budding transitions (type 1)

A typical budding transition is shown in Fig. 3. Starting at 25.3°C with a spherical shape under lateral stress, the vesicle first becomes a prolate ellipsoid, then a pear and finally a sphere with a small vesicle pointing to the outside. The ellipsoidal and pear shapes in the regime between 27.2°C and 40.9°C are stable. A further increase in temperature of 0.1 K to 41.0°C causes a sudden transition to an outside budded state. At this temperature the pear shapes become unstable. Further increasing the area-to-volume ratio formes a chain of vesicles. This process is shown below for POPC vesicles (cf. Fig. 10 *a*).

In case of recooling the budded vesicles we found three different types of behavior:

(*a*) The bud retracts suddenly after cooling down to between ≈ 10 and ≈ 30 K below the temperature where

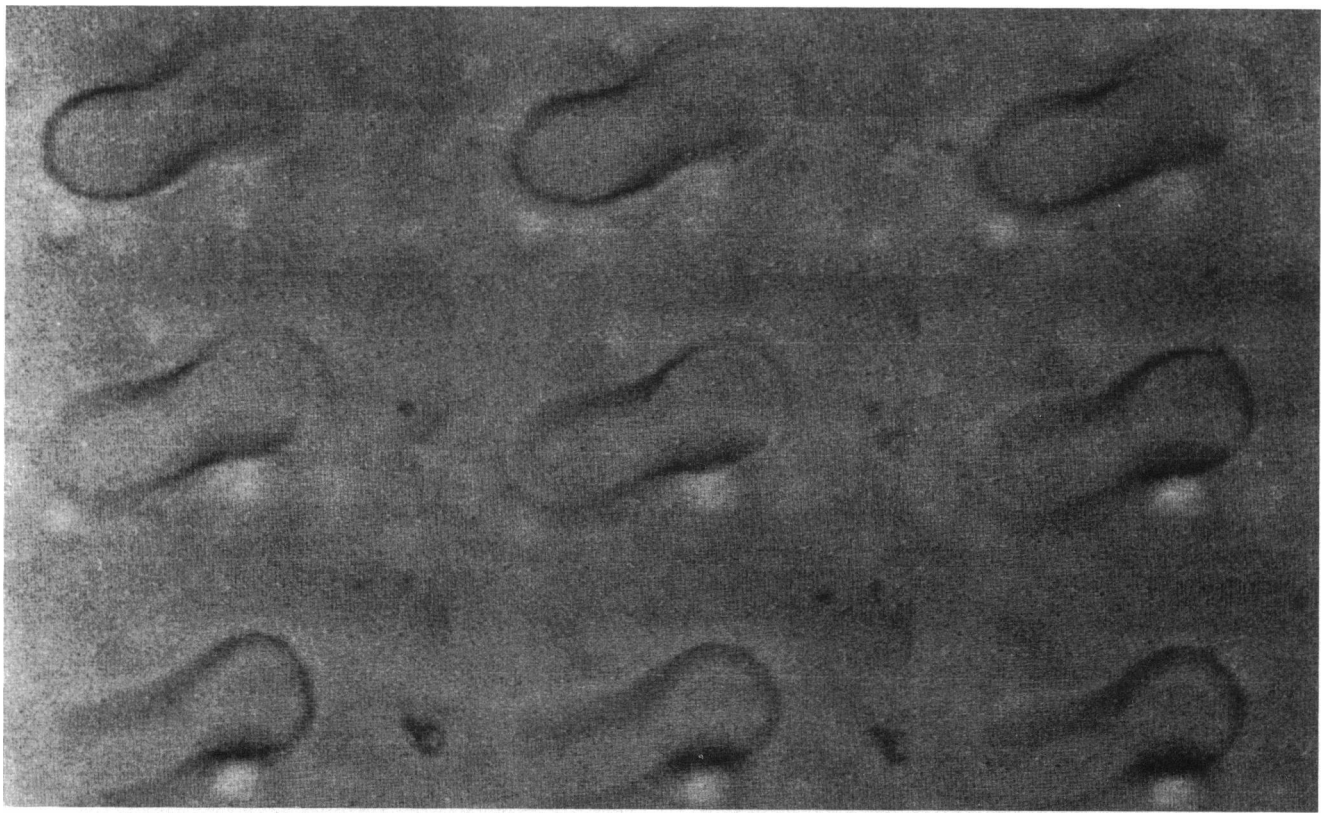

FIGURE 2 Example of determing the global structure of a vesicle by the variation of focus. It is easily seen that the vesicle exhibits a dumbbell shape.

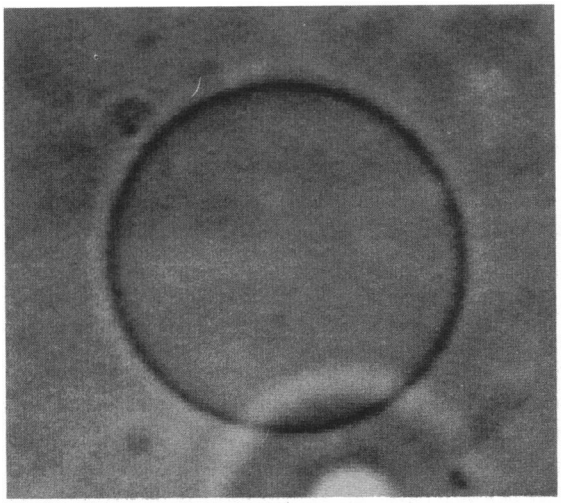

(1): T=27.2°C V=12200μm^3 A=2570μm^2

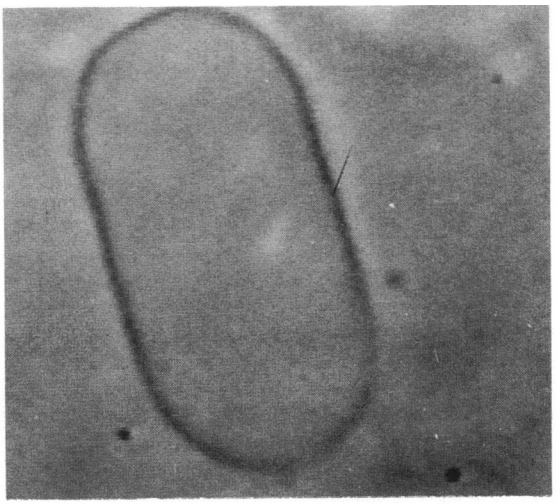

(2): T=36.0°C V=12200μm^3 A=2770μm^2

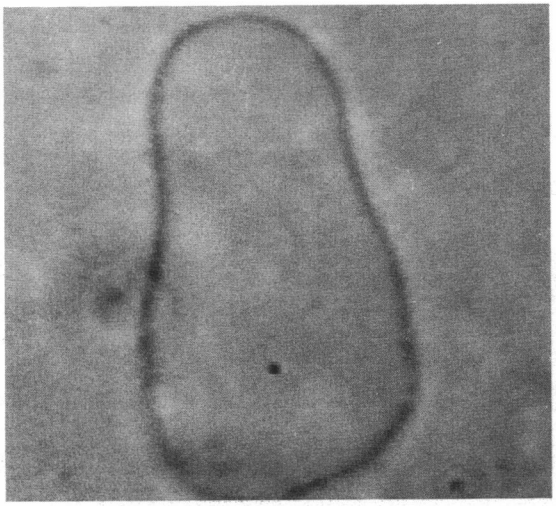

(3): T=37.5°C V=10800μm^3 A=2750μm^2

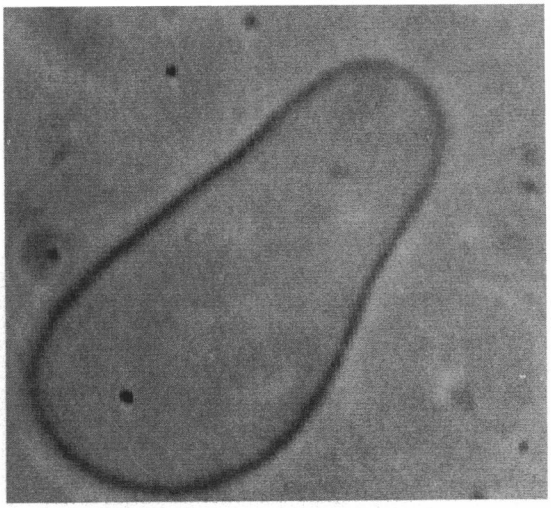

(4): T=39.1°C V=12000μm^3 A=2800μm^2

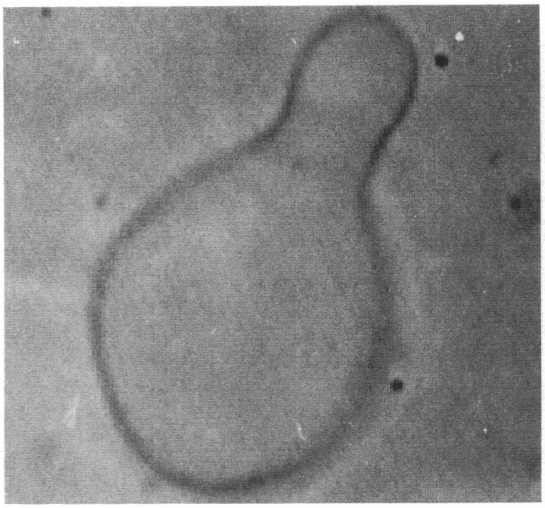

(5): T=41.0°C V=11900μm^3 A=2810μm^2

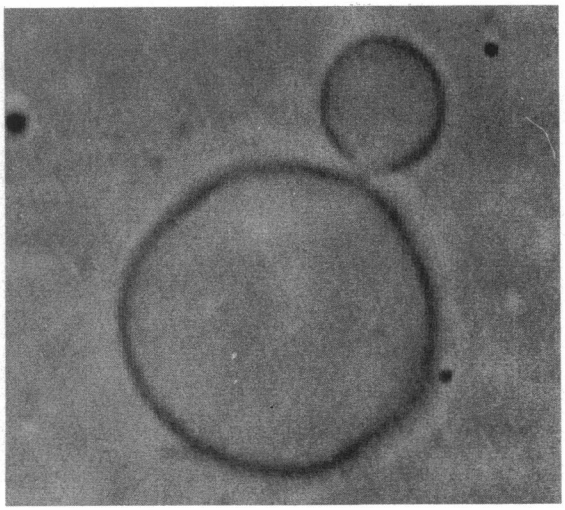

(6): T=41.0°C V=12000μm^3 A=2820μm^2

budding had occurred during the heating cycle. Then the vesicle assumes the shape of a prolate ellipsoid or a slightly pear-shaped state. The transition back to the spherical vesicle is completely reversible.

(*b*) A second type is widening of the neck between the two vesicles, followed by renarrowing of the neck and then formation of a smaller daughter vesicle. The transient widening of the neck is due to the lateral stress of the membrane caused by decreasing area. This happens several times during the cooling cycle as shown in Fig. 4. The shapes with the open neck seem to be unstable.

(*c*) A last possibility is shown in Fig. 5 *a* where a vesicle with a chain of small vesicles is cooled. This vesicle was originally spherical and the heating cycle was started at 27.9°C. Fig. 5 *a* shows that the number of vesicles of the chain is reduced in a step-wise manner from four to one between 35.6 and 27.2°C until a prolate ellipsoid is formed. At further decrease of the area, however, budding of the vesicle to the inside occurs. Thus the shape change is not completely reversible. The formation of an invagination suggests that the vesicle has lost some volume during the recooling. This is indeed verified by the parallel measurement of the volume, V, which is shown in Fig. 5 *b*. Between 36 and 27°C the volume is reduced by 8%. The loss in volume is large enough, that the reduced volume, v ($v := V/[4\pi/3\,(A/4\pi)^{3/2}]$), remains constant during the decrease of the area, A. Presumably, local pore formation took place during the cooling. Most likely, these instabilities occur at the temperatures where the number of small vesicles is reduced by one which may lead to a high strain at the necks between the vesicles or at the tip of the outermost vesicle.

The first possibility happens for vesicles with one daughter vesicle, if the recooling is done very slowly. In some cases the outside budded vesicle remained stable until reaching the onset of the L_α-P_β-transition. In this case fission of the daughter vesicle occurred. If the cooling is performed fast, the second possibility occurs for vesicles with one daughter vesicle. Loss of volume could only be observed for chains of vesicles. The step-wise reduction of the daughter vesicles in the type 3 seems to be consistent with the view introduced in reference 5.

FIGURE 3 Typical budding transition (type 1) of a DMPC vesicle in pure water. The temperatures, the volume, and the values for the area are given below the figures. In the temperature regime between 27.2° and 40.9°C the vesicle shapes are stable. At 41.0°C the vesicle shape becomes unstable going over into the budded limiting shape. From 98 examined DMPC vesicles 35 vesicles showed this behavior. This transition happens if lateral stress is exerted to the vesicle before heating.

Transitions from discocyte via stomatocyte to inside budded shape (type 2)

Fig. 6 shows such a kind of shape change. The discocytes are generated by heating nearly spherical vesicles which are slightly flickering (that is tension free) passing first oblate ellipsoidal shapes. Both the discocytes and the stomatocytes are stable with respect to small temperature changes up to 42.3°C (frame 1 to 20 in Fig. 6). However, at further increase of the excess areas after small temperature changes of 0.1°C, the stomatocyte invagination suddenly becomes unstable going over into an inside budded vesicle. In the case of Fig. 6 this happens at 42.4°C. When the inside budded vesicle was cooled again two types of behavior were found: either the small vesicle retracts with a temperature hysteresis or volume is lost owing to pore formation. Interestingly, the ratio of the radii of the two vesicles does not change during the latter process.

Reentrant dumbbell-pear-shaped-dumbbell transitions (type 3)

An example of a reentrant transition is shown in Fig. 7. Initially the vesicle is in a dumbbell shape exhibiting a large excess area of $A_{excess} = 79\ \mu m^2$. Increasing the temperature first leads to an asymmetric pear shape which changes back again to the symmetric dumbbell shape at a further increase of the excess area. Both transitions are continuous. The observed shapes are stable and the transition is completely reversible.

Blebbing transitions and abrupt tether formation (type 4)

An example of this type of shape changes is shown in Fig. 8 *a*. It has been observed with initially spherical vesicles (image 1 of Fig. 8 *a*). Increase of the temperature (by 3.8°C) leads first to quasispherical vesicles which flicker slightly. After further heating by 4.8°C the shape becomes edgy and flickering stops (cf. image 2 of Fig. 8 *a*). At 37.1°C tethers protrude immediately from the edges and their radii widen rapidly. Moreover, with a slight time delay blebs are forming at the smooth areas of the vesicle shell. After heating further by several degrees ($\approx$5.5°C) the blebs and tethers widen more and more and eventually a large flaccid vesicle is formed as shown in Fig. 8 *b*. Finally an inside budded state is reached (cf. Fig. 8 *c*). It should be emphasized firstly that the transition of Fig. 8 *a* occurs close to the spherical shape after a small increase of the excess area ($\sim$6.7% in Fig. 8 *a*). Secondly, this type of transition is a

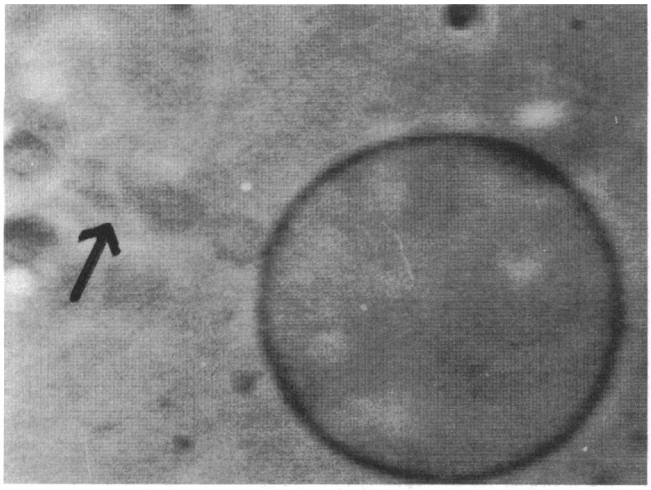

(1): T=35.6°C

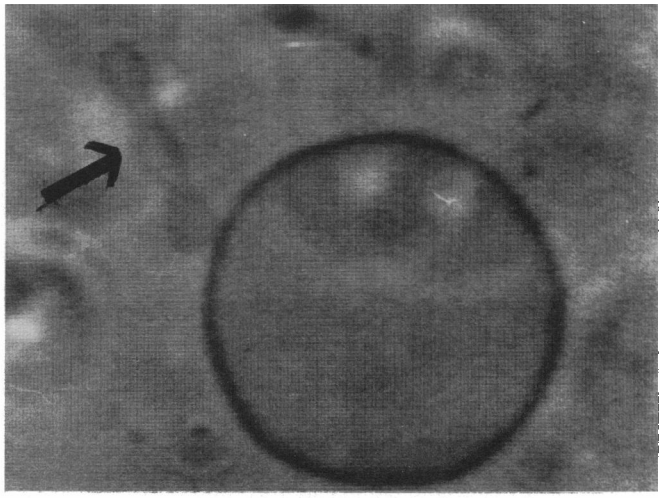

(2): T=34.0°C

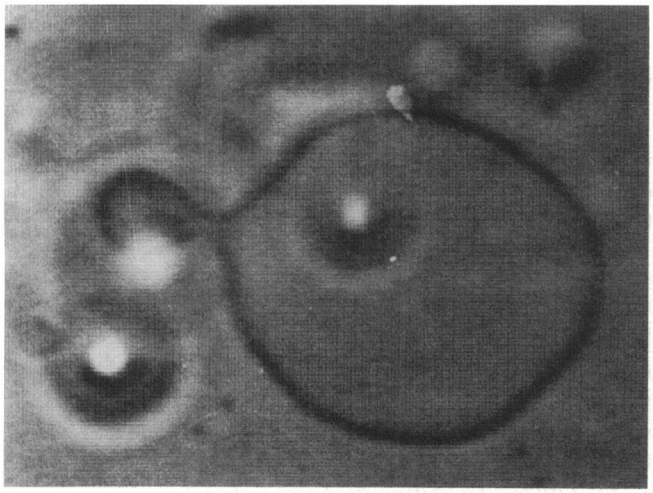

(3): T=27.2°C

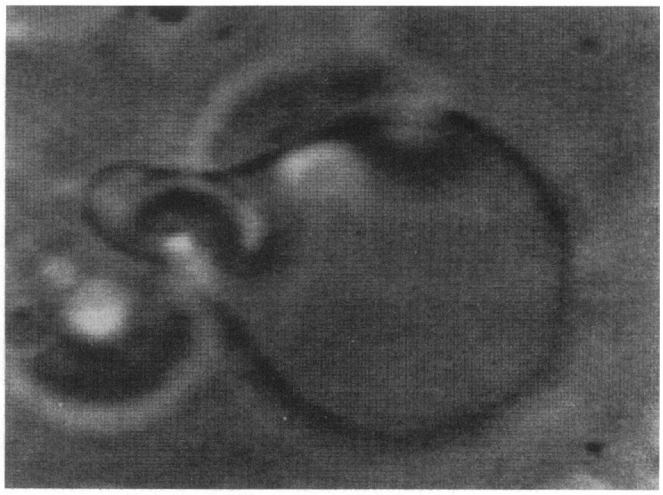

(4): T=25.9°C

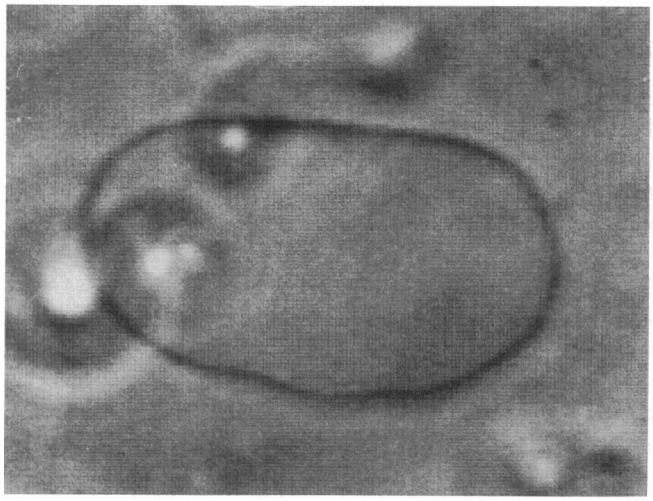

(5): T=25.2°C

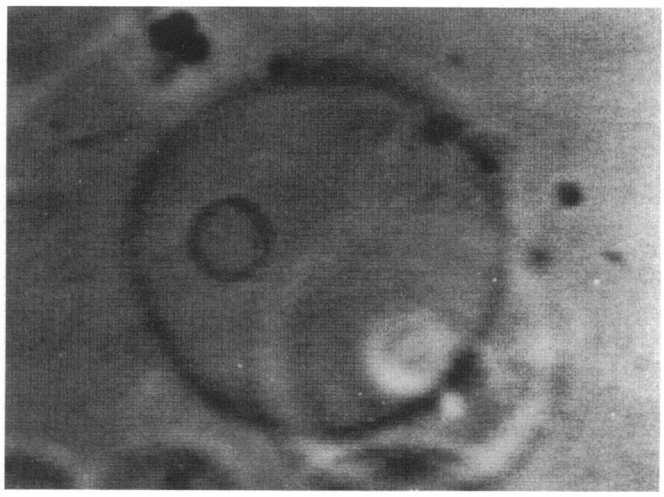

(6): T=24.5°C

very seldom event for DMPC. We observed this transition only twice.

Prolate ellipsoid-discocyte-stomatocyte transitions (type 5)

A surprising shape transition of DMPC vesicles in pure water is shown in Fig. 9. The vesicle was heated from an initially prolate ellipsoidal shape which passed into a dumbbell shape at first. At 43.7°C a sudden transition into a discocyte takes place whereas further increase of A_{excess} leads to a stomatocyte and finally to an inside budded state. As follows from the simultaneous measurement of the area, A, and the volume, V, of the vesicle the dumbbell-discocyte transition is accompanied by a loss of material since both A and V decrease by 6% and 20%, respectively. This example demonstrates clearly both that shape transitions of symmetric bilayer vesicles are determined by an area-to-volume ratio change, and that measurements of area and volume are essential in studies of shape changes. The thermal expansitivity of $\alpha = 7.3 \times 10^{-3}\ K^{-1}$ following from the A-T-plot (before and after the sudden decrease) corresponds well with the values measured by the micropipette technique (11).

Budding transitions to the inside of POPC vesicles in pure water

At increasing temperatures, POPC vesicles show in general sphere-to-oblate ellipsoid-to-stomatocyte-to-inside budded transitions, which are similar to the type 2 transitions of DMPC vesicles. The main differences between the shape changes of POPC and DMPC vesicles are that the temperature interval between the initial spherical and the budded states is much smaller for POPC and that the diameters (2–4 μm) of the daughter vesicles are smaller than for DMPC. Further increasing the excess area of inside budded vesicles leads to two different types of behavior: either the inside vesicle evolves into a chain of vesicles (shown in Fig. 10 *a*) or the additional excess area causes subsequent blebbing at other locations leading to inverted echinocyte-like shapes as shown in Fig. 10 *b*.

We also looked at the effect of solutes instead of pure water on the shape transitions or of different aqueous solutions in inside and outside medium at equal osmotic pressure.

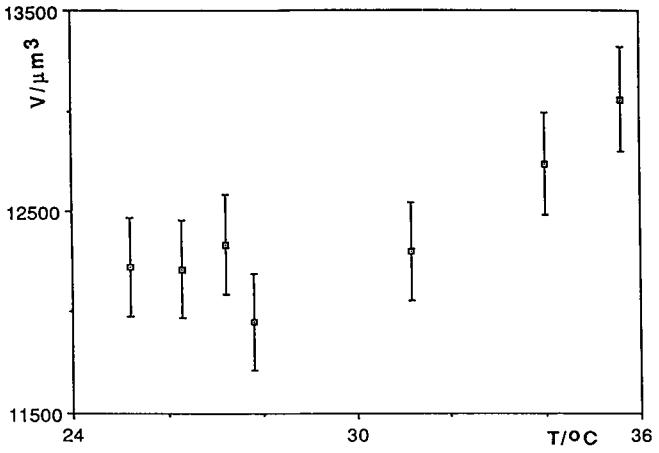

FIGURE 4 (*a*) Shape transition induced by decreasing the excess area of an outside budded DMPC vesicle. Note the discontinuous reduction of the number of vesicles of first four images. The bright spots are due to air bubbles which migrate in the outer compartment of the measuring chamber. The arrow indicates the pearl string of vesicles. (*b*) Measurements of the volume of the vesicle as a function of temperature shown in Fig. 4 *a*. Note that there is a loss in volume due to the transient pore formation at decreasing temperature.

Effect of solutes

To study the influence of solutes (symmetrically distributed at the outside and the inside) on shape transitions of DMPC and POPC the above experiments were performed in solutions of NaCl, Hepes, and inositol. These studies can be summarized as follows: the same types of shape transitions as described above are observed provided the osmolarity is small (≤ 20 mosm). At higher osmolarities, however, only one type was observed for both DMPC and POPC: at increasing excess areas, spherical vesicles go over into prolate ellipsoids which elongate with increasing A_{excess} until tube-like structures are formed. It is interesting to note that electrically induced blebbing of cells is also impeded above 20 mosm (12).

DMPC or POPC vesicles containing cholesterol (~ 30 mol%) exhibit transitions into inside budded shapes even in the presence of 180 mosm inositol.

Finally we should mention that in sucrose solutions even at smaller concentrations (inside and outside) one occassionally observes the formation of very thin threads extending into the vesicle interior. In this case the vesicle exhibited a spherical nonflickering shape in the whole region of temperature variation.

Spontaneous curvature-induced (continuous) shape changes

To explore the effect of asymmetrically distributed solutes on the observed shape changes and on the continuity of these changes the following experiment was performed: DMPC vesicles were swollen in a 200 mosm inositol solution. Then the outer solution was slowly exchanged by dialysis against a 100 mM (200 mosm) solution of NaCl. In this way the osmolarity C =

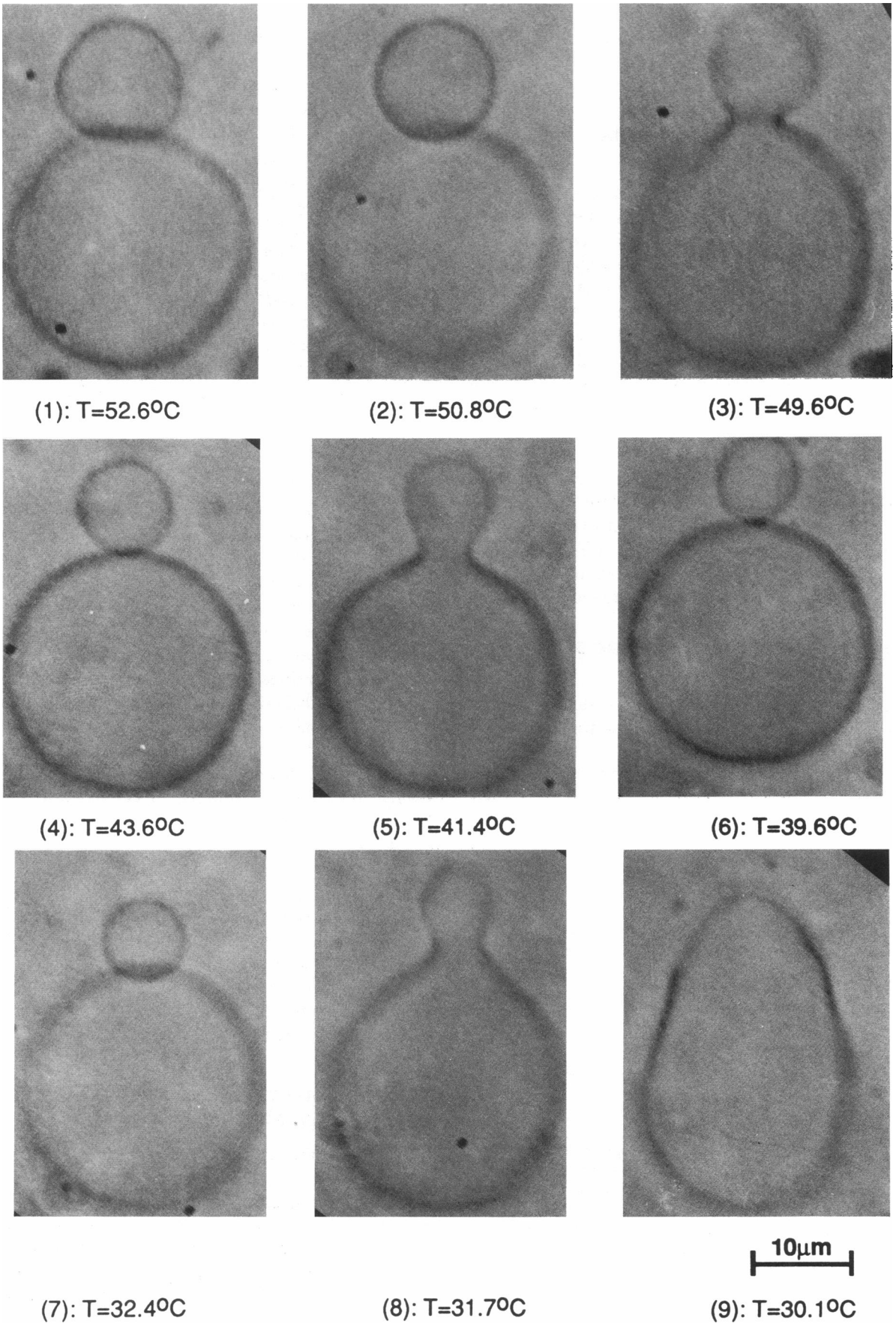
(1): T=52.6°C
(2): T=50.8°C
(3): T=49.6°C
(4): T=43.6°C
(5): T=41.4°C
(6): T=39.6°C
10μm
(7): T=32.4°C
(8): T=31.7°C
(9): T=30.1°C

$C_{Na+} + C_{Cl-} + C_{inositol} = 200$ mosm (C_i: concentrations of the different ingredients) at the inside and outside of the vesicle was kept equal. The increase of the NaCl concentration as a function of time was measured in a separate experiment as follows: the measuring chamber was filled with Millipore water. The NaCl concentration was increased slowly by pumping a 100 mM NaCl solution through the dialysis tubes. The osmolarity was measured with an osmometer (micro-osmometer 3MO; Advanced Instruments, Needham Heights, MA). In this way the change in NaCl concentration with time in the inner compartment was determined. The constancy of the osmolarity, C, was demonstrated in a similar dialysis experiment by filling the chamber with a 200 mosm inositol solution instead of Millipore water. At the beginning the vesicle exhibits an ellipsoidal (oblate) shape. The increase of the NaCl content of the outer medium causes the formation of an invagination which deepens at increasing NaCl content (cf. Fig. 11). This cup forming process could possibly be explained by assuming that inositol molecules are solved in the two monolayers of the vesicle. Under this assumption the decrease of the inositol concentration at the outside also causes a decrease of the inositol molecules solved in the outer monolayer. Thus, an asymmetry between the two monolayers occurs which could be the cause of the cup forming process.

DISCUSSION OF SHAPE CHANGES

The present study shows that shape transitions caused by increase of membrane excess area may be divided into two classes. In the first class (denoted above as type 1 to 3) the shapes such as dumbbells, stomatocytes, discocytes, and pears are stable (with respect to small temperature changes) over an extended range of the excess area. Eventually the stomatocytes or pears undergo a sudden transition into a limiting shape (inside or outside budded vesicles) within a very small temperature intervall (of ≤ 0.1°C). In the second class (denoted above as type 5) tethers and blebs shoot out of the vesicle shell even after a small increase in area of some 6.7%. We found that before this instability the vesicles assumed a rigid, slightly polygonal shape.

Our observations suggest that the type of transition depends on the pretreatment. The type 1 transition occurs if the spherical vesicle was kept for some time (~30 min) under high lateral tension. The remarkable difference in the behavior of vesicles of POPC and DMPC shows that for a given change in excess area the transition depends also on the lipid structure. Some of the shape transitions can also be induced at constant excess area by variation of the surrounding medium of the bilayers causing a change in spontaneous curvature.

FIGURE 5 Shape transition caused by cooling an outside budded vesicle. Starting at 52.6°C the neck between the bleb and the mother vesicle opens transiently for the first time at 49.6°C which is shown in the first three pictures and again at three lower temperatures, namely 45.7°, 41.4°, and 35.3°C. The bleb disappears at 31.7°C.

Models of shape transitions

Two models of vesicle shapes have been proposed: the original spontaneous curvature model (6) and the bilayer coupling model (2). These models are correlated by a Legendre transformation. However, they predict different paths of shape changes with increasing area. In agreement with a previous study (1) and as shown in a recent short communication (8) our experiments can best be explained by the bilayer coupling model with exception of the instabilities close to the limiting shapes. In this model the shape is determined by the minimum bending energy

$$G_{el} = \tfrac{1}{2} K_c \int (c_1 + c_2)^2 dA^{in} \qquad (1)$$

(K_c: bending elastic modulus, $c_1 + c_2$: mean curvature) under the constraint that the volume, V, and the area of the inner monolayer, A^{in}, are fixed. The key assumption is that lipid exchange (flip-flop) between the inner and outer monolayers is so slow that it can be neglected and that therefore the area difference between the two monolayers $\Delta A = A^{ex} - A^{in}$ is fixed. Owing to this coupling hypothesis the integration in Eq. 1 is performed over the inner monolayer only. The area difference can be expressed in terms of the mean curvature as $\Delta A = d \int (c_1 + c_2)\, dA^{in}$ provided the distance d ($\approx \frac{1}{2}$ bilayer thickness) between the center of the monolayers is small ($d \ll [c_1 + c_2]^{-1}$).

Axisymmetric shapes of minimum curvature energy have been numerically calculated originally by Zeks and Svetina (2) and more recently by Seifert et al. (4) as a function of the reduced volume, v, and reduced area difference, Δa, defined as

$$v := V/[(4\pi/3)\,(A^{in}/4\pi)^{3/2}]$$
$$\text{and} \quad \Delta a := \Delta A/[8\pi d\,(A^{in}/4\pi)^{1/2}]. \qquad (2)$$

For spherical shapes $v = 1$ and $\Delta a = 1$. The reduced volume, v, is another measure for the excess area. The extended v-Δa-phase diagram of minimum bending energy calculated by Seifert et al. (4) is reproduced in Fig. 12. It is limited by outside budded shapes for $\Delta a > 1$ and by inside budded shapes for $\Delta a < 1$. Most of the

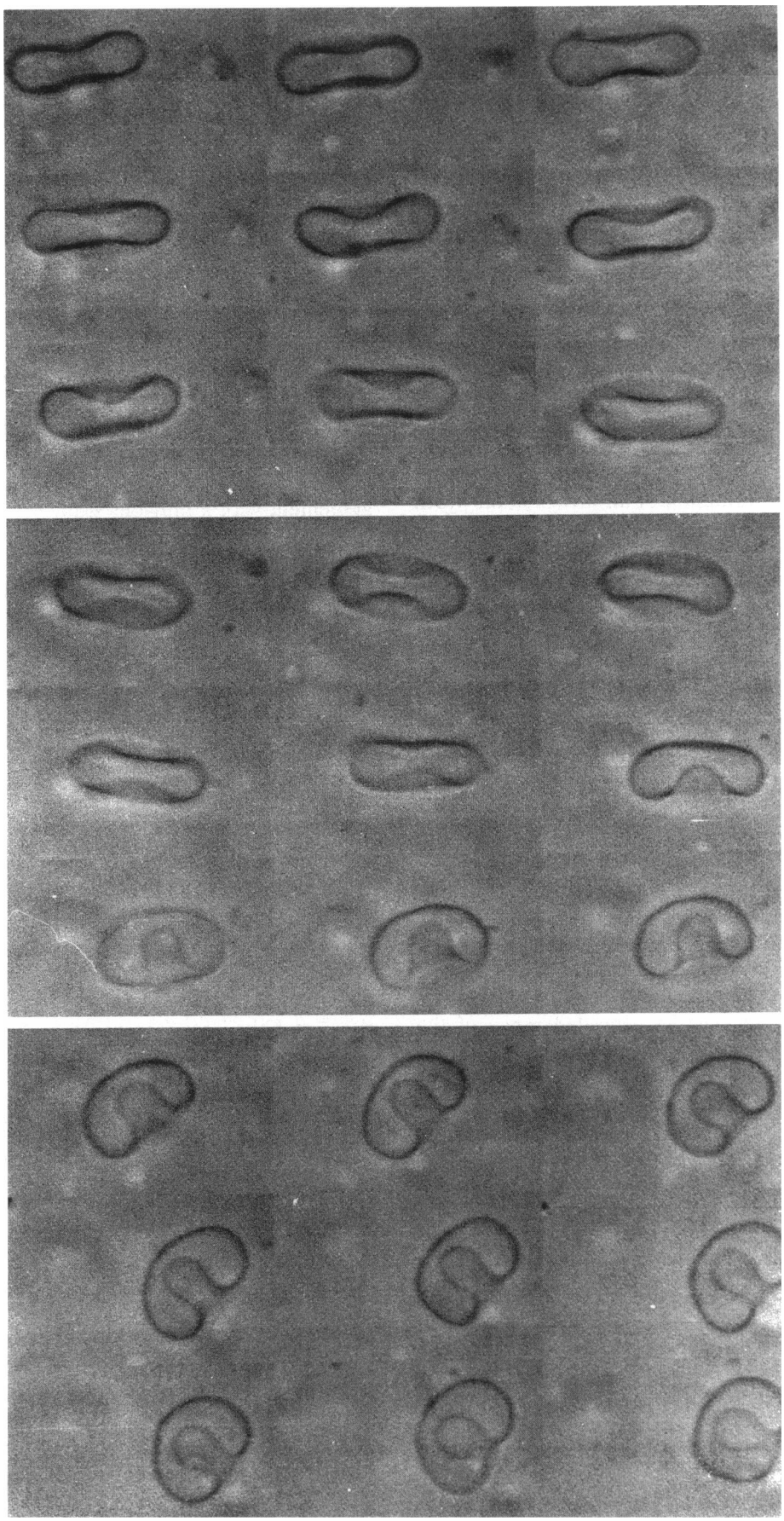

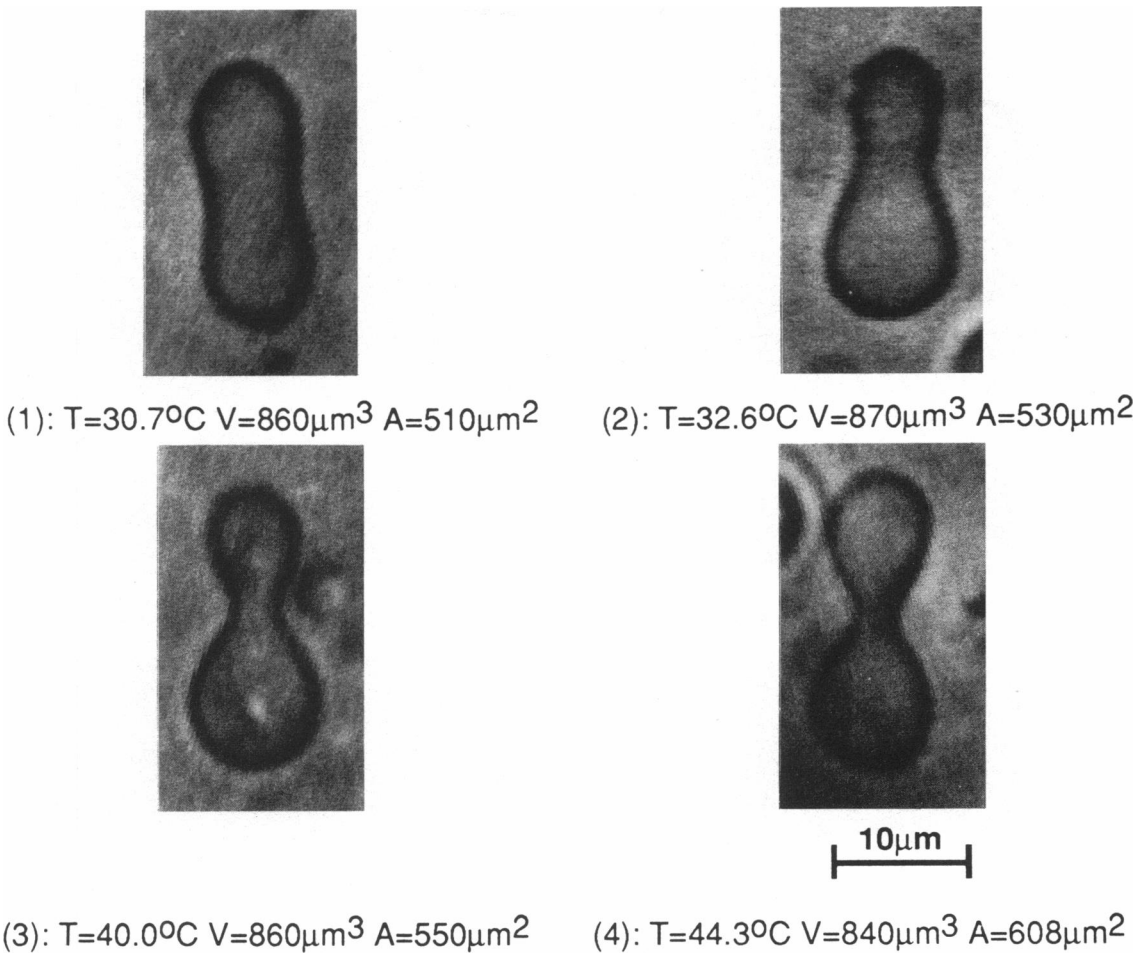

FIGURE 7 Example of a reentrant transition from a dumbbell to a pear-shaped state of a DMPC vesicle in pure (Millipore) water. All the shapes of this continuous transition are stable. The temperatures, the volume, and the areas are given below the pictures. This type of transition occurred with 29 vesicles.

experimentally observed shapes lie easily within this phase diagram, with exception of the chain of vesicles protruding from the mother vesicle (Fig. 4 *a* and Fig. 10 *a*), the inverted echinocytes (Fig. 10 *b*) and the irregular shapes shown in Fig. 8, *a* and *b*. The shapes in Fig. 4 *a* and Fig. 10 *a* lie beyond the limiting shapes of the budded vesicles.

FIGURE 6 Discocyte-stomatocyte transition of a DMPC vesicle in pure water observed at increasing temperature. The temperature was varied from 41.9° to 42.4°C at a rate of 0.02°C per image. The set of images starts at the left top and ends at the right bottom. The area varies from 1,370 μm^2 at 41.9°C to 1,380 μm^2 at 42.4°C and the volume is 3,200 μm^3. In a separate stepwise heating cycle we found that all the shapes are stable up to a temperature of 42.3°C. We observed this type of transitions with 31 vesicles.

Asymmetric thermal expansivity of monolayers as driving force of shape changes

As shown in the preliminary communication (8) the observed shape transitions of symmetric bilayer membranes can be explained by assuming that the thermal expansivities of the inner (α^{in}) and outer monolayer (α^{ex}) exhibit a small difference, γ. This assumption may be expressed (8) as

$$\alpha^{ex} := \frac{1}{A^{ex}} \frac{dA^{ex}}{dT} = (1 + \gamma)\alpha^{in}. \quad (3)$$

Neglecting the small thermal expansivity of the enclosed water and assuming that the thermal expansivity of d is given by $-\alpha^{in}/2$ (13), the reduced area difference, Δa,

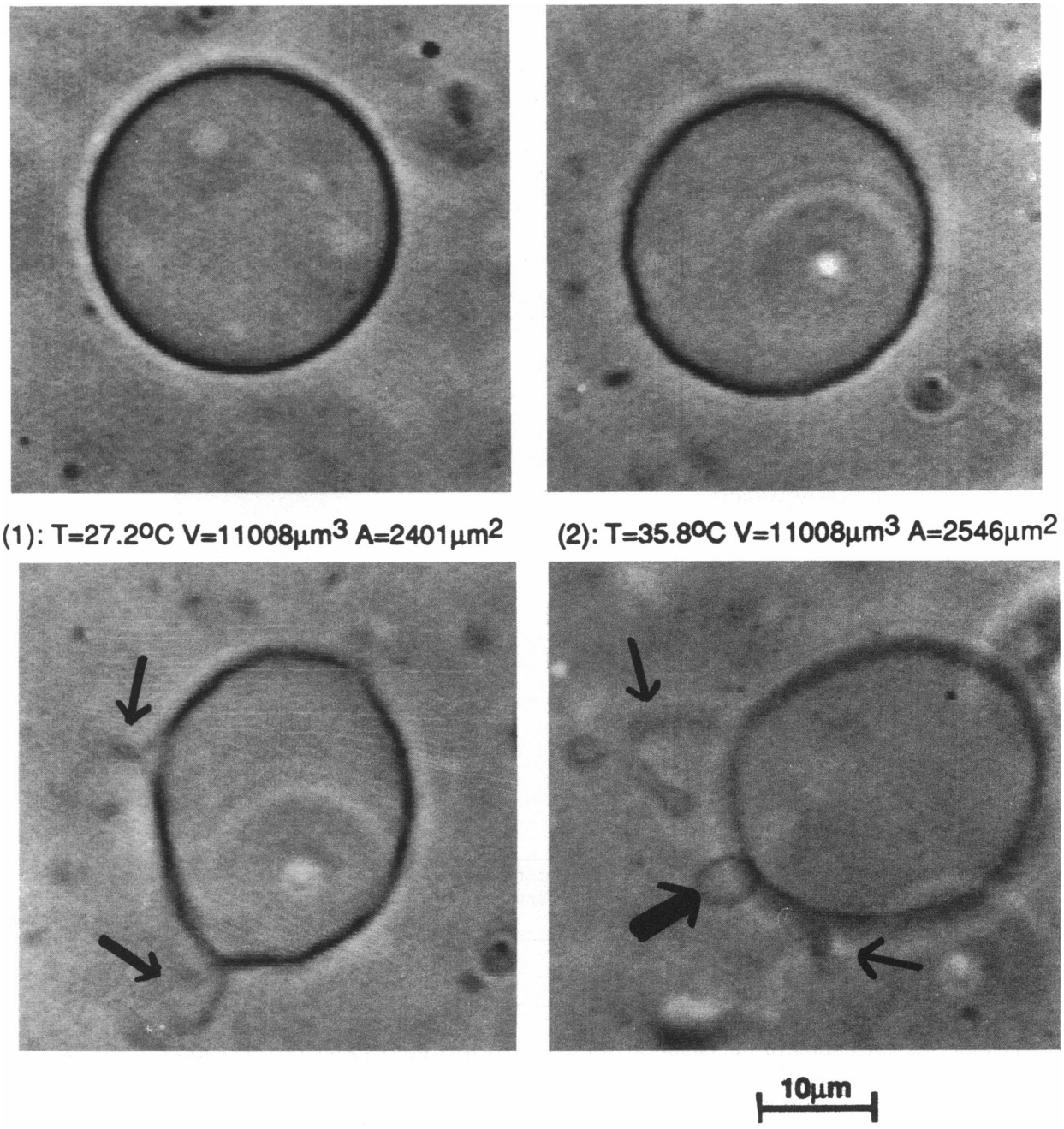

and the reduced volume, v, depend on the temperature as follows:

$$\Delta a(T) = \frac{\{A^{ex}(T_0) \exp[\gamma\, \alpha^{ex}\, (T - T_0)] - A^{in}(T_0)\}}{8\pi\, d(T_0)\, (A^{in}(T_0)/4\pi)^{1/2}} \cdot \exp[(-3/2)\, \alpha^{in}]$$

$$\text{and} \quad v(T) = v(T_0) \exp[(-3/2)\, \alpha^{in}\, (T - T_0)], \tag{4}$$

where $v(T_0)$ and $\Delta a(T_0)$ parameterize the initial shape at temperature $T = T_0$. By eliminating $(T - T_0)$ from these equations the change of the reduced area difference can be expressed as a function of v:

$$\Delta a(v) = \left(\frac{v(T_0)}{v}\right)^{2/3} \left[\Delta a(T_0) + b\left(\left(\frac{v(T_0)}{v}\right)^{2\gamma/3} - 1\right)\right]$$

$$\text{with} \quad b := A^{ex}(T_0)/\{8\pi\, d(T_0)\, [A^{in}(T_0)/4\pi]^{1/2}\}. \tag{5}$$

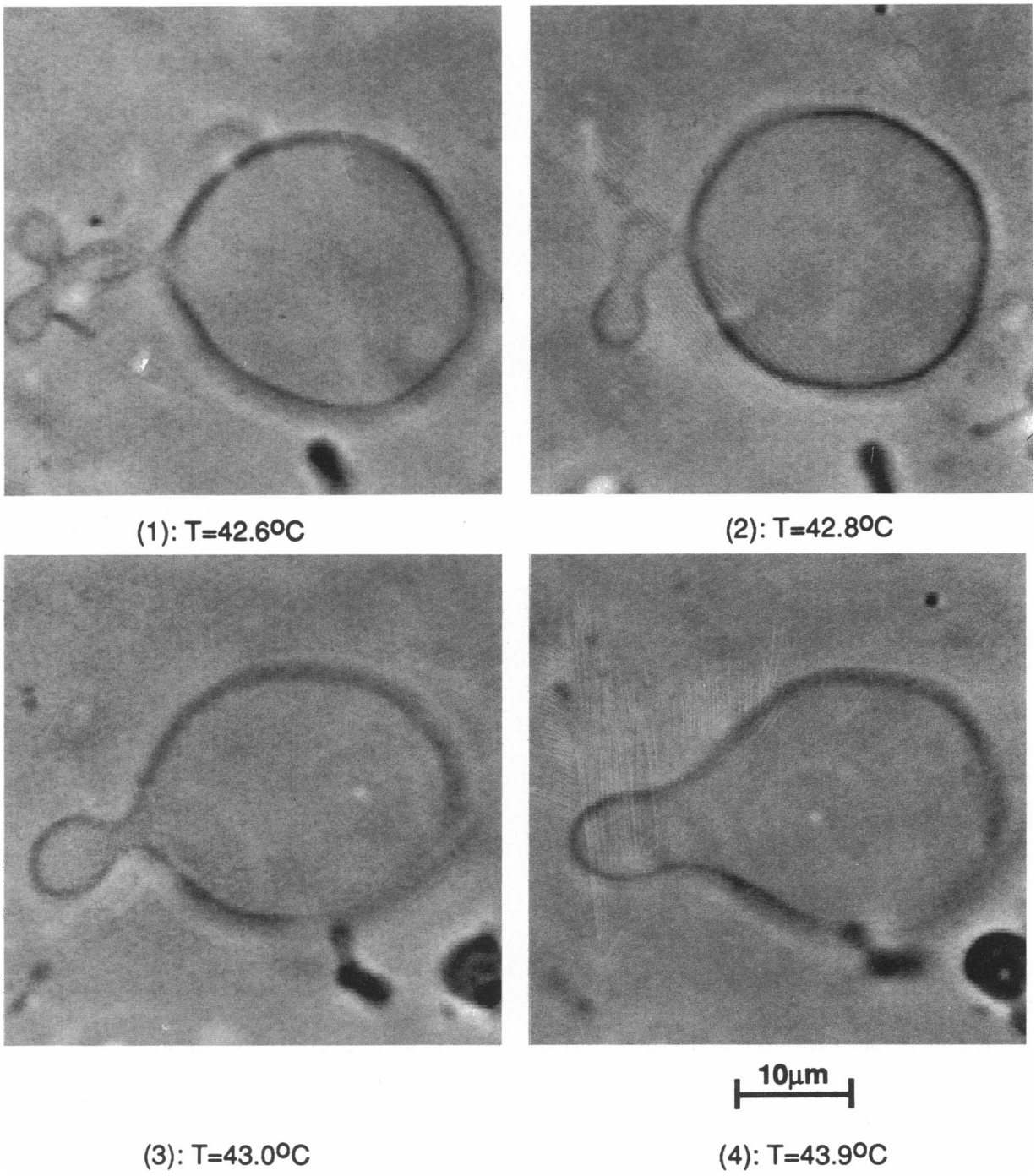

FIGURE 8 (*a*) Discontinuous transition of a DMPC vesicle in pure water caused by an increase of the area of only 6.7%. Temperature, area, and volume are indicated at the bottom of each image. Instead of measuring the values of the surface area (which is not possible for these irregular shapes) they are calculated by assuming a thermal expansivity of $6 \cdot 10^{-3}\,K^{-1}$. The tubes are indicated by thin arrows and the bleb by a thick arrow. This type of transition took place only twice. (*b*) Evolution of the branched tube shown at the upper left corner of Fig. 8 *a* with increasing temperature. (*c*) Final shape of the vesicle shown in Fig. 8 *b* reached at a temperature of 44.2°C. The picture shows a stomatocyte seen from the top.

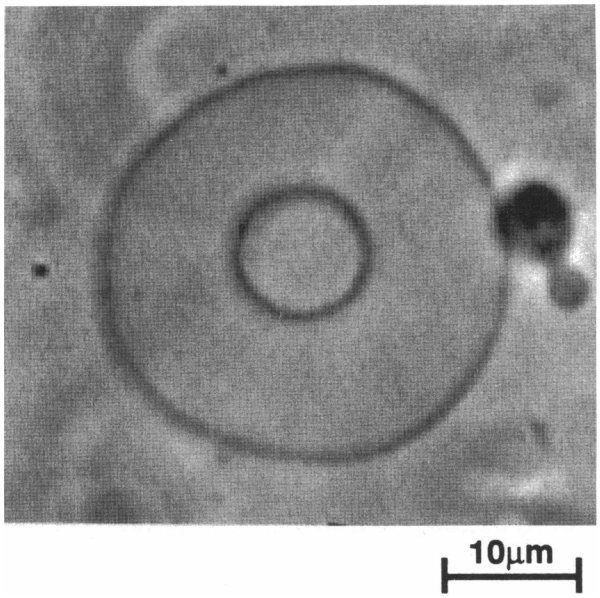

FIGURE 8 (continued)

Eq. 5 represents trajectories within the phase diagram which are passed through at varying temperature and which depend on the expansivity difference γ. Owing to the large value of b, a small thermal expansivity difference γ may have already drastic effects on the trajectory passed (and thus on the accessible shape transitions). For vesicles of 20 μm diam and a bilayer thickness of 5 nm one obtains $b = 10^3$ and γ values of the order of 10^{-3} are sufficient to influence the shape transitions drastically. For demonstration a few trajectories are presented as dashed lines in Fig. 12 which have been determined by comparison of the calculated and the observed shape changes.

Comparison with experiments

The exploration of the temperature-induced shape changes in terms of the phase diagram is impeded by the fact that it is not possible to control $\Delta a(T_0)$ and γ experimentally to pass through a selected trajectory given by Eq. 5. $\Delta a(T_0)$ depends on the initial state (e.g., area-to-volume ratio) and on the pretreatment of the vesicles. The latter determines γ, the expansivity difference parameter. This is at least strongly suggested by our finding that γ assumes positive values if (spherical) vesicles are subjected to lateral stress before starting the heating cycle, e.g., by cooling the vesicles some degrees below the temperature at which they become spherical.

To compare our experiments with the theory, all four parameters, $\Delta a(T_0)$, $v(T_0)$, γ and b, of Eq. 5 characterizing the trajectory of the shape change have to be determined. For that purpose vesicles with symmetric shapes (e.g., prolate ellipsoids) were selected. V and $A(T_0)$ are determined as described above and $v(T_0)$ and b are than obtained by Eq. 2 and Eq. 4. The initial reduced area difference, $\Delta a(T_0)$, is determined by comparison of the experimental and theoretical shapes. $v(T_{max})$ is obtained with Eq. 4 and $\Delta a(T_{max})$ is fitted to the experimental shape, which finally determines the value of γ.

In Fig. 13 we compare the experimentally observed shapes with the theoretical shapes calculated for the phase trajectories indicated as dashed lines in Fig. 12. Clearly good agreement is observed with the exception of the observed instabilities close to the limiting shapes. Perhaps these instabilities could be explained by including the Van der Waals attraction to the bilayer coupling theory. The comparison of calculated and observed shapes shows: the transition of type 1 (spherical-to-pear-to-outside budded shape) requires a positive γ value, the reentrant transition (type 3) is expected for γ values close to zero and the discocyte-stomatocyte transition (type 2) for negative γ values.

As already noted above, the bilayer coupling model is related to the spontaneous curvature model by a Legendre transformation, and the question arises whether the observed shape changes can also be explained by the latter model. A phase diagram based on this concept has been calculated by Seiffert et al. (4). The same family of vesicle shapes as for the model of Svetina and Zeks is obtained. However, the order of the shape transitions as well as the shape stability predicted by the two models differ remarkably. For the following reasons, we conclude that our observations can be better explained in terms of the bilayer coupling model:

(*a*) The spontaneous curvature model (3–5) predicts that pear shapes and stomatocytes are only stable close to the outside or inside budded limiting shapes. This is in contradiction to our finding that both pears and stomatocytes are stable over a large range of the excess area and become unstable only if one approaches the excess area close to the values characteristic for the limiting shapes. In particular, our finding of stable pear and dumbbell shapes at the reentrant transition (type 3) and the continuity of this shape change contrasts with the result of the Helfrich model which predicts a discontinuous pear-dumbbell transition.

(*b*) To explain the budding transition (type 1) by the Helfrich model, a large reduced spontaneous curvature, c_0 ($c_0 = C_0/\{A^{in}/4\pi)^{1/2}\} \approx 5$–$6$, C_0: spontaneous curvature), has to be assumed which appears very unprobable for DMPC vesicles in pure water. The strange behavior observed during recooling the outside or inside budded vesicles may be explained by Van der Waals interactions arising between the opposing bilayers in the narrow

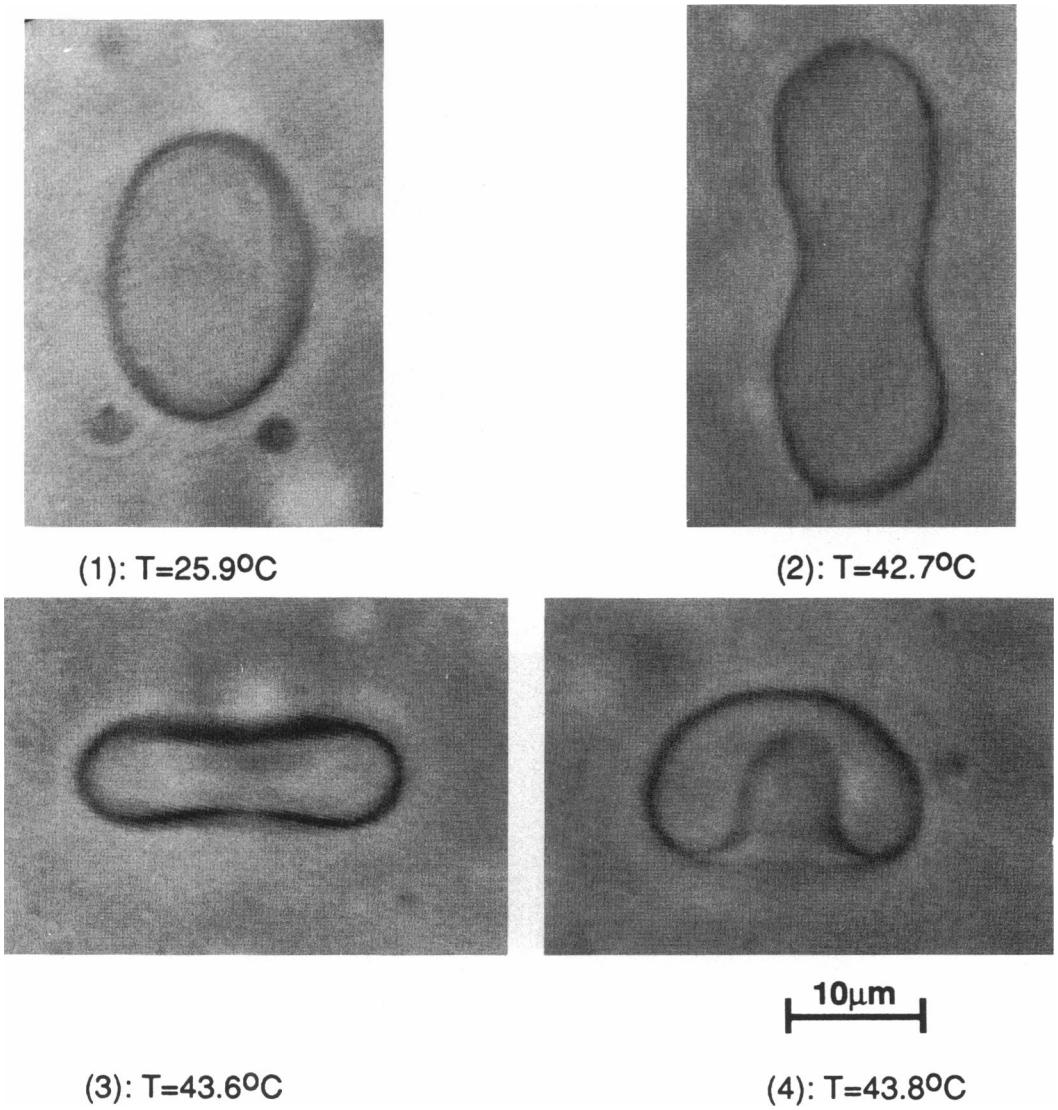

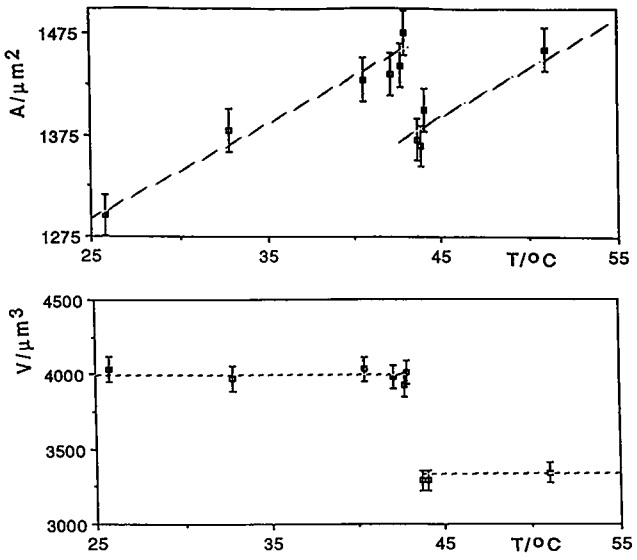

FIGURE 9 Example of a shape transition of a DMPC vesicle in ion free water accompanied by an instability (loss of material). (*a*) Sequence of transient shapes of a vesicle forming initially a prolate ellipsoid with a volume of 4,000 μm^3 and an area of 1,490 μm^2. The discocyte shape is stable at $T \geq 43.6°C$. (*b*) Temperature dependence of area and volume of the vesicle of Fig. 9 *a*. Note that the thermal expansivity is the same above and below the point of instability.

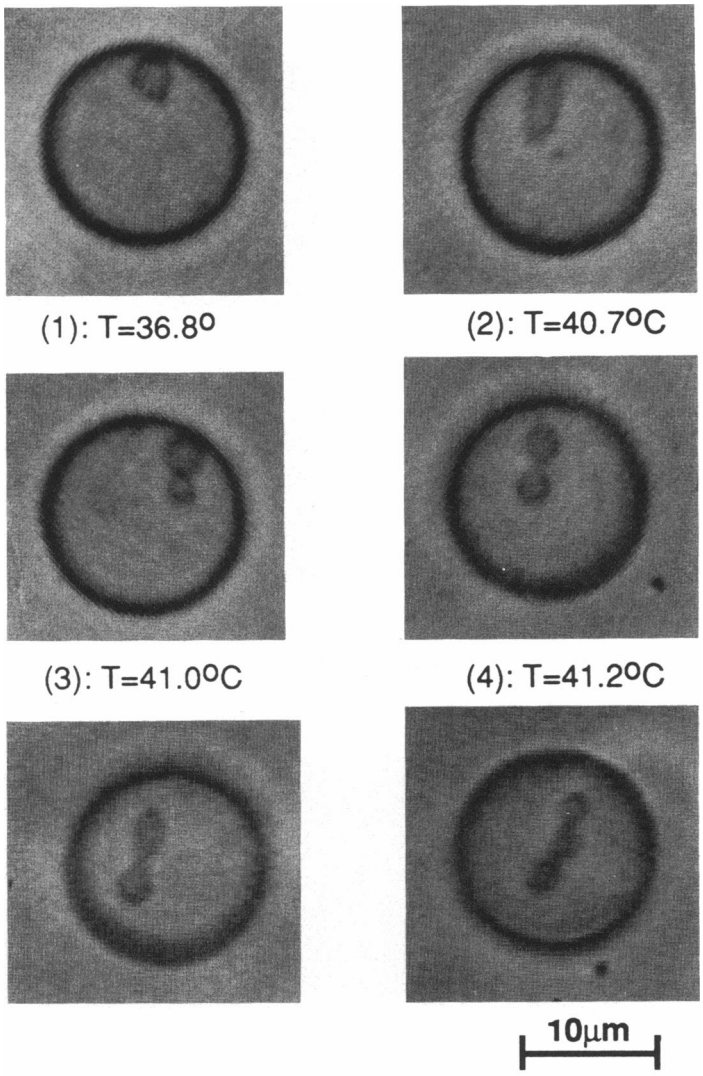
(1): T=36.8°
(2): T=40.7°C
(3): T=41.0°C
(4): T=41.2°C
10μm
(5): T=43.4°C
(6): T=44.2°C

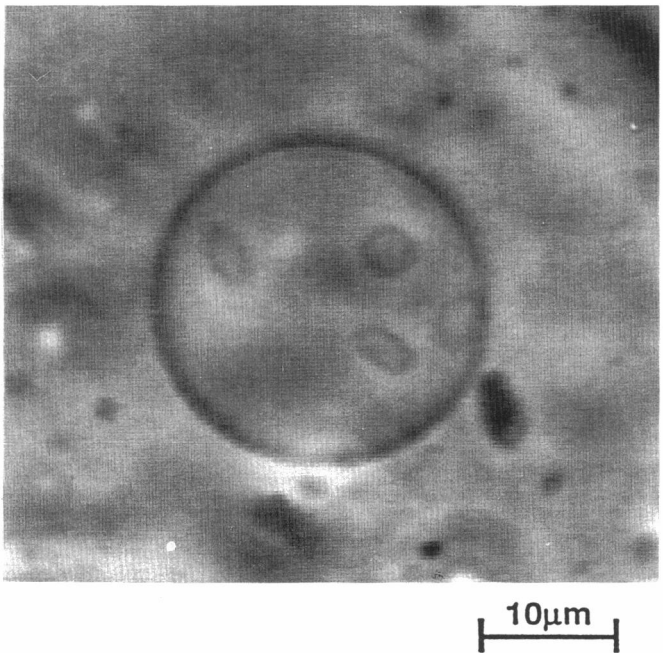
10μm

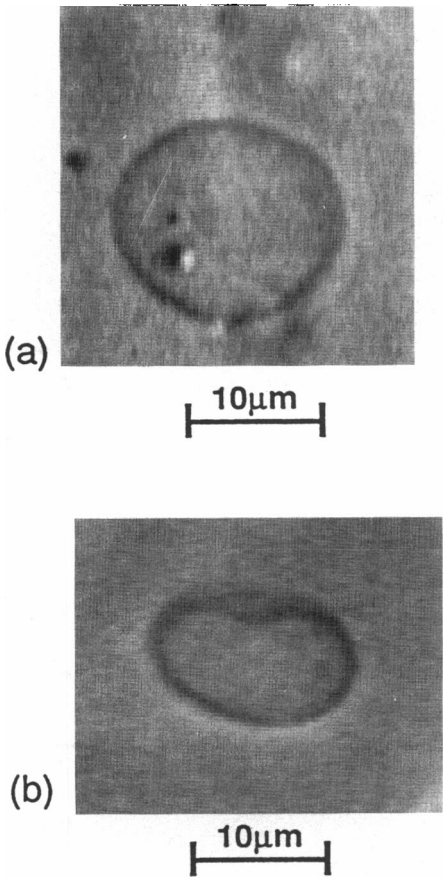

FIGURE 11 Example of a spontaneous curvature induced shape change at a constant temperature (29.4°C). DMPC was swollen in 200 mosm inositol. Then the inositol was continuously replaced at the outside by a (isoosmolar) 100 mM NaCl solution via the dialysis tubes. (*a*) DMPC vesicle at 29.4°C in a 200 mM inositol solution at the inside and the outside. (*b*) Shape change after replacement of outer medium by 178 mM inositol and 11 mM NaCl solution.

necks linking the small daughter vesicles with each other.

It should be pointed out that the spontaneous blebbing and tether formation (type 4) cannot be explained with any of the two models. One possible explanation is that the bilayer membrane of the spherical vesicle is folded exhibiting tethers and folds and that these protrusions adhere to the vesicle shell and are thus invisible. The folding happens most probably during the swelling of the vesicles. Heating could then cause unbinding of the tethers and folds which could explain their sudden appearance. This explanation is also supported by the fact that the increase in area by thermal expansion is too small to form as many tethers and blebs as observed. Folded structure could also explain the edgy shape of the vesicles since the membrane exhibits a three times higher bending modulus at those parts where the tethers or folds adhere. This causes regions of different curvature and edges at the border of these regions.

The sphere-to-oblate ellipsoid-to-stomatocyte-to inside budded transitions of POPC can be identified as type 2 transitions ($\gamma < 0$). Thus they can be explained in terms of the bilayer coupling model. The difference to DMPC vesicles is that the slopes of the phase trajectories are steeper which means that the absolute γ values are larger for POPC. This is indicated by the smaller temperature intervals, in which the transitions occur, and the smaller size of the daughter vesicles for POPC.

FIGURE 10 (*a*) Formation of a chain of vesicles starting with a inside budded POPC vesicle in ion free (Millipore) water. The temperatures are indicated below the pictures. (*b*) POPC vesicle at 41.3°C in pure water showing the shape of an inverted echinocyte.

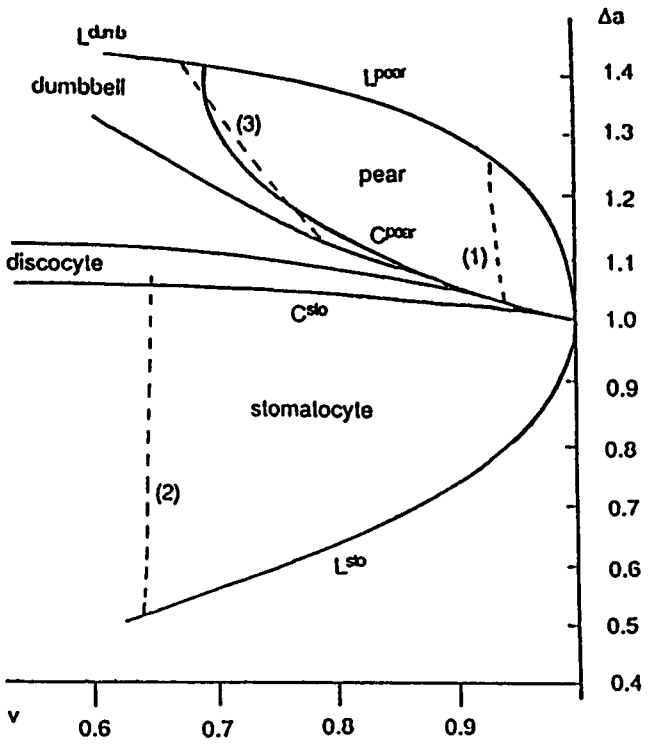

FIGURE 12 Phase diagram of minimum bending energy vesicle shapes calculated by the bilayer coupling approach (8) as a function of the reduced volume, v, and area difference, Δa, between inner and outer monolayer. The phase boundaries denoted by C^{sto}, C^{pear} define two continuous transitions at which the up-down symmetry is broken and the outer solid lines L^{pear}, L^{dumb}, L^{sto} define limiting shapes. Note that for large v values the dumbbell regime contains prolate ellipsoids and the discocyte regime contains oblate ellipsoids. The dashed lines show experimentally observed trajectories which can be described by Eq. 5 for various values of γ (1: $v_0 = 0.94$, $\Delta a_0 = 1.03$, $\gamma = 0.057$, $b = 1500$; 2: $v_0 = 0.65$, $\Delta a_0 = 1.03$, $\gamma = -0.29$, $b = 1000$; 3: $v_0 = 0.78$, $\Delta a_0 = 1.15$, $\gamma = 0.0017$, $b = 640$).

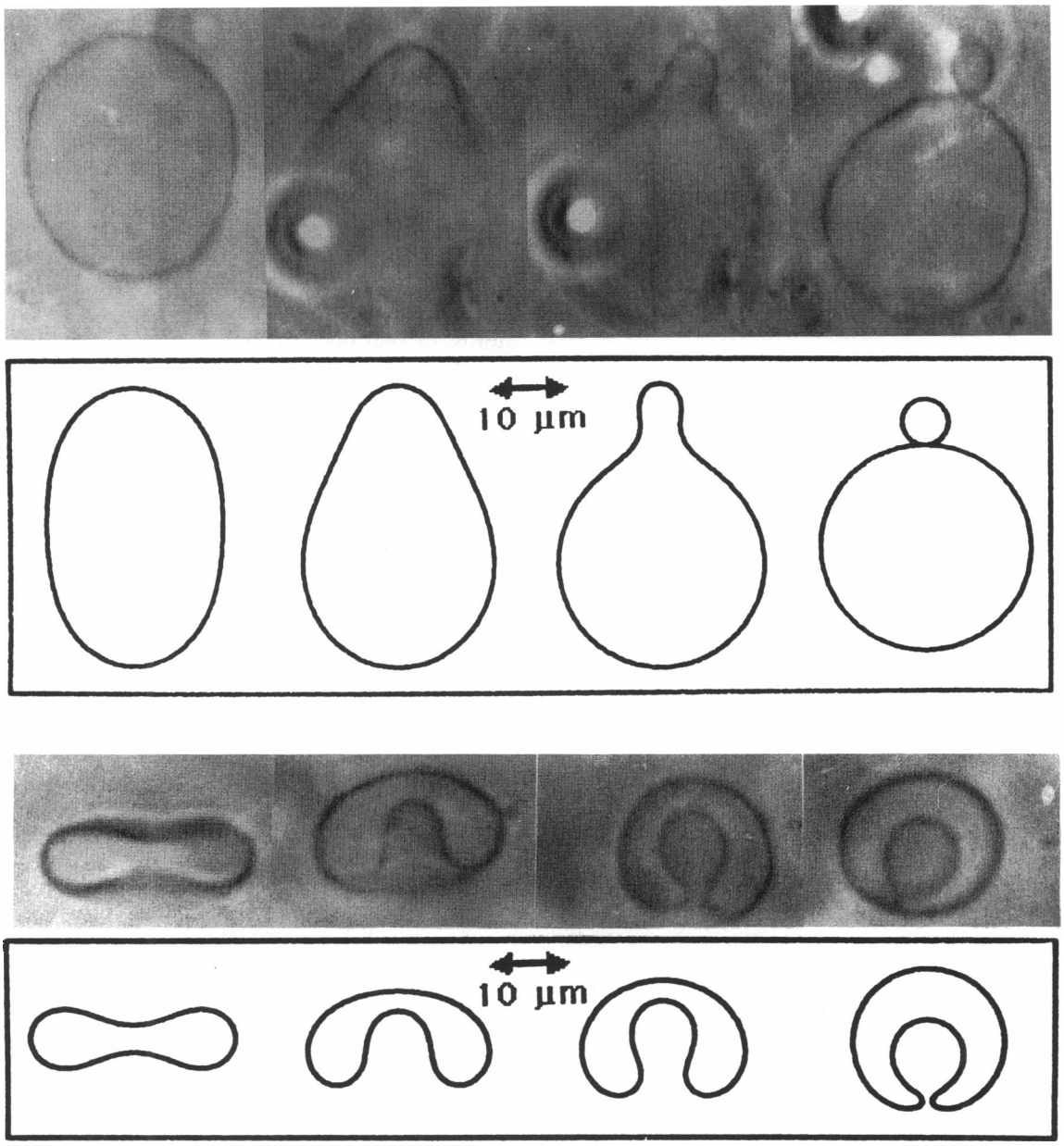

The larger γ values even compensate the fact that $v(T_0)/v$ (see Eq. 4) increases more slowly with the temperature in the case of POPC because of the smaller thermal expansivity of POPC ($\alpha^{POPC} = 3.5 \times 10^{-3}K^{-1}$, $\alpha^{DMPC} = 6 \times 10^{-3}K^{-1}$). This example shows that the γ values depend on the lipid structure.

Possible microscopic molecular origin of bilayer asymmetry γ

What could be the origin of the different thermal expansivities of the two monolayers? One possibility could be impurities such as lysolipids asymmetrically distributed between inside and outside. A second and more likely possibility is that the asymmetry is introduced during swelling or equilibration under lateral tension. For example, if an initially flaccid vesicle is cooled below the temperature where it just becomes spherical the lateral pressure could cause a driven lipid transfer between the monolayers. Indeed, we showed recently that even a small lateral pressure may decrease the half-time of lipid flip-flop from some 10 h to <1 h (14). If the vesicle is heated again after equilibration it might contain an excess of lipid in one of the monolayers as a possible cause of the positive value of γ. To be more general, let us consider a lateral pressure difference

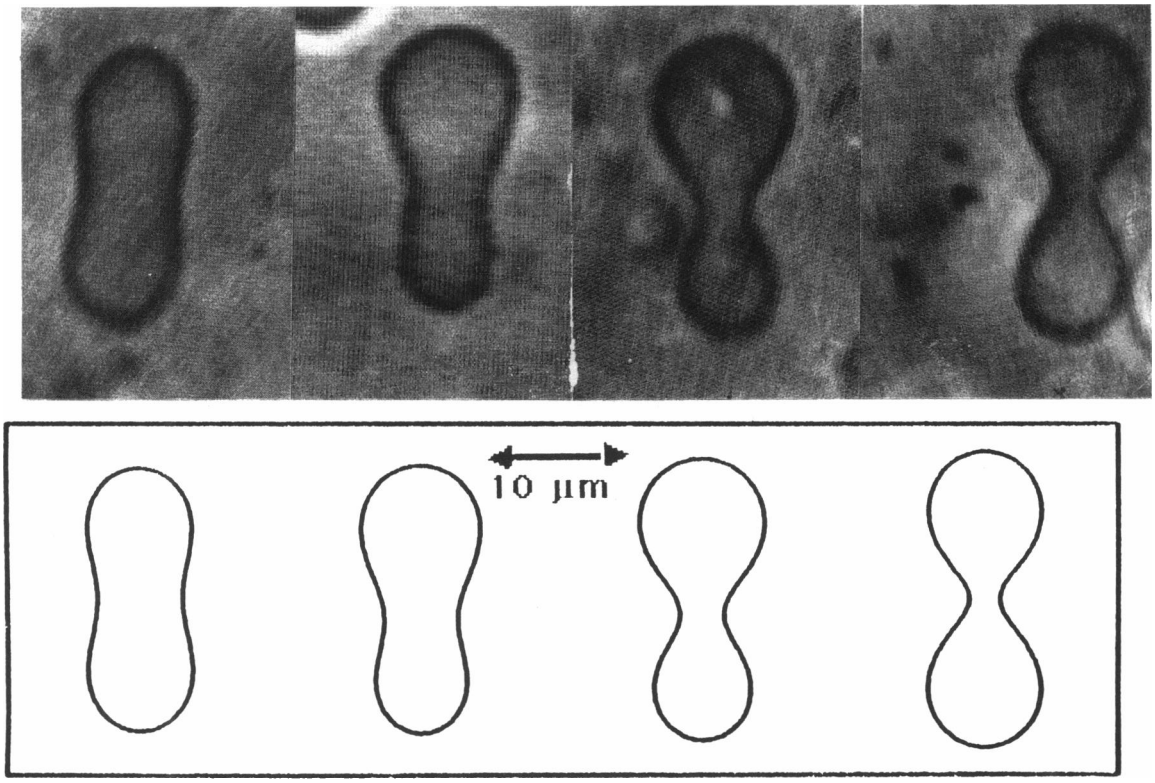

FIGURE 13 Comparison between the experimental and theoretical shapes (8) according to the phase trajectories shown in Fig. 12. (*a*) Budding transition belonging to the trajectory (1) ($\gamma = 0.057$). (*b*) Discocyte-stomatocyte transition described by trajectory (2) ($\gamma = -0.29$). (*c*) Dumbbell-pear-dumbell transition belonging to the trajectory (3) ($\gamma = 0.0017$).

between the two monolayers. The relative change in area with temperature for the monolayer is then (i = in, ex)

$$\frac{1}{A^i}\frac{dA^i}{dT}dT = \left[\frac{1}{A^i}\frac{\partial A^i}{\partial T}\right]_\pi dT + \kappa_i \frac{d\pi^i}{dT}dT, \qquad (6)$$

where κ_i is the (isothermal) lateral compressibility of the monolayer i and π^i is the lateral pressure of the monolayer i. The asymmetry, γ, could thus also be a consequence of different compressibilities or changes in pressure with temperature.

Finally, even if the description of the different phase trajectories with the help of an asymmetry in the thermal expansivities seems to be reasonable, we are aware of the possibility that these phase trajectories could be explained by some other mechanism.

Helpful discussions with U. Seifert, R. Lipowsky, W. Helfrich, S. Svetina, B. Zeks, and E. Evans are gratefully acknowledged. We are grateful to R. Lipowsky, K. Berndl, and U. Seifert for providing us with a copy of their calculations of the phase diagram obtained by the bilayer coupling model.

The work was supported by the Deutsche Forschungsgemeinschaft through the Sonderforschungsbereich SFB 266.

Received for publication 21 February 1991 and in final form 10 June 1991.

REFERENCES

1. Duwe, H. P., H. Engelhardt, and E. Sackmann. 1986. Membrane bending elasticity and its role for shape fluctuations and shape transformations of cells and vesicles. *Faraday Discuss. Chem. Soc.* 81:281–290.
2. Svetina, S., and B. Zeks. 1989. Membrane bending energy and shape determination of phospholipid vesicles and red blood cells. *Eur. Biophys. J.* 17:101–111.
3. Wiese, W., and W. Helfrich. 1990. Theory of vesicle budding.
4. Seifert, U., K. Berndl, and R. Lipowsky. Shape transformations of vesicles: phase diagram for spontaneous curvature and bilayer coupling model.
5. Miao, L., B. Fourcade, M. Rao, M. Wortis, and R. K. P. Zia. 1990. Equilibrium budding and vesiculation in the curvature model of fluid lipid vesicles.
6. Deuling, H. J., and W. Helfrich. 1976. The curvature elasticity of fluid membranes: a catalogue of vesicle shapes. *J. Physique.* 37:1335.
7. Evans, E., and W. Rawics. 1990. Entropy-driven tension and

bending elasticity in condensed fluid membranes. *Phys. Rev. Lett.* 64:2094.

8. Berndl, K., J. Käs, R. Lipowsky, E. Sackmann, and U. Seifert. 1990. Shape transformations of giant vesicles: extreme sensitivity to bilayer asymmetry. *Europhys. Lett.* 13:659–664.
9. Kwok, R., and E. Evans. 1981. Thermoelasticity of large lecithin billayer vesicles. *Biophys. J.* 35:637–652.
10. Duwe, H. P., J. Käs, and E. Sackmann. 1990. Bending elastic moduli of lipid bilayers: modulation by solutes. 51:945–962.
11. Evans, E., and D. Needham. 1986. Giant vesicle bilayers composed of mixtures of lipids, cholesterol and polypeptides. *Faraday Discuss. Chem. Soc.* 81:267–280.
12. Gass, G. V., and L. V. Chernomordik. 1990. Reversible large-scale deformations in the membranes of electrically-treated cells: Electroinduced bleb formation. *Biochem. Biophys. Acta.* 11:1023.
13. Cevc, G., and D. Marsh. 1987. Phospholipid Bilayers. John Wiley and Sons, New York. 364 pp.
14. Bayerl, T. M., C. F. Schmidt, and E. Sackmann. 1988. Kinetics of symmetric and asymmetric phospholipid transfer between small sonicated vesicles studied by high-sensitivity differential scanning calorimetry, NMR, electron microscopy, and dynamic light scattering. *Biochemistry.* 27:6078–6085.